

## Two-Dimensional Bimetallic Carbonyl Cluster Complexes with New Properties and Reactivities

Richard D. Adams,<sup>\*,†</sup> Qiang Zhang,<sup>†</sup> and Xinzheng Yang<sup>\*,†</sup>

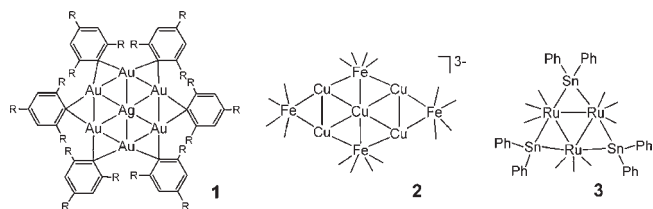
<sup>†</sup>Department of Chemistry and Biochemistry, University of South Carolina, Columbia, South Carolina 29208, United States

<sup>‡</sup>Molecular Graphics and Computation Facility, College of Chemistry, University of California, Berkeley, California 94720, United States

**S** Supporting Information

**ABSTRACT:** The new electron-rich, anionic, planar cluster complex  $[\text{IrRu}_6(\text{CO})_{23}]^-$ , **5**, isolated as a PPN salt,  $\text{PPN} = [\text{Ph}_3\text{PNPPH}_3]^+$ , has been synthesized and characterized crystallographically. The complex exhibits unusual absorption and emission properties. Computational analyses have been performed to explain its metal–metal bonding and electronic properties. Anion **5** reacts with  $[\text{Ph}_3\text{PAu}][\text{NO}_3]$  to yield the uncharged planar complex  $\text{Ru}_5\text{Ir}(\text{CO})_{20}\text{AuPPh}_3$ , **6**, by metal atom substitution.

Two-dimensional (2D) bimetallic carbonyl cluster complexes having six or more metal atoms are interesting simply because there are so very few of them.<sup>1–4</sup> The majority of the planar 2-D cluster complexes contain significant numbers of metal atoms from the copper subgroup having closed ( $d^{10}$ ) subshells, e.g. **1** and **2**:  $[\text{Au}_6\text{Ag}(\mu\text{-}2,4,6\text{-C}_6\text{H}_2\text{R}_3)_6]^+$ , **1**,  $\text{R} = \text{CHMe}_2$ ;  $[\text{Cu}_5\text{Fe}_4(\text{CO})_{16}]^{3-}$ , **2**; and  $\text{Ru}_3(\text{CO})_9(\mu\text{-SnPh}_2)_3$ , **3**, etc., as shown below where the CO ligands in **1**, **2**, and **3** are represented only as lines from the metal atoms.<sup>2–4</sup>



In recent studies, our group has been synthesizing bimetallic carbonyl cluster complexes for use as precursors to new selective heterogeneous nanocluster hydrogenation catalysts.<sup>5–7</sup> We have found that the planar cluster complex **3** can be fixed and imaged intact on a monolayer of  $\text{SiO}_2$ .<sup>8</sup> 2D clusters are of interest in catalysis because all of the metal atoms lie on the surface. 2D metal clusters have also been found to exhibit interesting magnetic properties.<sup>9</sup> 2D molecular clusters may also exhibit interesting physical and reactivity properties that depend on their sizes and shapes. For example, it has been shown that one can add a series of  $\text{Pt}(\text{P-}t\text{-Bu}_3)$  groups to the  $\text{Ru-Sn}$  bonds of complex **3** to form an extended 2D structure.<sup>4</sup> The addition of each platinum grouping progressively modifies the absorption of light by the  $\text{Ru}_3\text{Sn}_3$  cluster. We have now prepared a new 2D transition metal carbonyl cluster that may form the basis for a series of new complexes that also exhibits interesting optical and

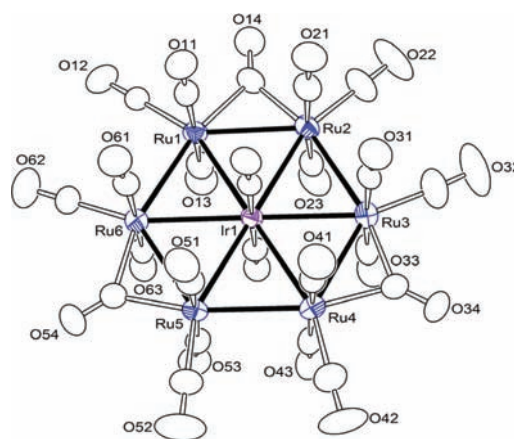


**Figure 1.** An ORTEP diagram of cluster anion  $[\text{IrRu}_6(\text{CO})_{23}]^-$ , **5**, showing 40% thermal probability. Selected interatomic bond distances (Å) are as follow:  $\text{Ir}(1)\text{--Ru}(1) = 2.8774(8)$ ,  $\text{Ir}(1)\text{--Ru}(2) = 2.8945(8)$ ,  $\text{Ir}(1)\text{--Ru}(3) = 2.8728(8)$ ,  $\text{Ir}(1)\text{--Ru}(4) = 2.9021(8)$ ,  $\text{Ir}(1)\text{--Ru}(5) = 2.8585(8)$ ,  $\text{Ir}(1)\text{--Ru}(6) = 2.9045(8)$ ,  $\text{Ru}(1)\text{--Ru}(2) = 2.8884(11)$ ,  $\text{Ru}(1)\text{--Ru}(6) = 2.9068(10)$ ,  $\text{Ru}(2)\text{--Ru}(3) = 2.8942(11)$ ,  $\text{Ru}(3)\text{--Ru}(4) = 2.8712(11)$ ,  $\text{Ru}(4)\text{--Ru}(5) = 2.8744(11)$ ,  $\text{Ru}(5)\text{--Ru}(6) = 2.8777(10)$ .

reactivity properties that may be traced to its structure and bonding.

The reaction of  $[\text{PPN}][\text{Ir}(\text{CO})_4]$  ( $\text{PPN} = [\text{Ph}_3\text{PNPPH}_3]^+$ ) with  $\text{Ru}_3(\text{CO})_{12}$  in equimolar amounts has been reported to yield the anionic tetranuclear cluster complex  $[\text{IrRu}_3(\text{CO})_{13}]^-$ , **4**, which has been shown to have a tetrahedral shape.<sup>10</sup> Interestingly, however, when  $[\text{PPN}][\text{Ir}(\text{CO})_4]$  was allowed to react with 2 equiv of  $\text{Ru}_3(\text{CO})_{12}$ , the new violet monoanionic cluster complex  $[\text{IrRu}_6(\text{CO})_{23}]^-$ , **5**, is formed and was isolated as its PPN salt in 91% yield.<sup>11</sup> An ORTEP diagram of the molecular structure of anion **5** is shown in Figure 1. All seven metal atoms lie in a plane (max deviation = 0.043(1) Å) with the iridium atom in the center circumscribed by a hexagonal ring of six ruthenium atoms. The six Ir–Ru distances range from 2.8585(8) to 2.9045(8) Å and are significantly longer than those found in **4** (ave 2.75 Å).<sup>10</sup> The Ru–Ru distances are all similar, range 2.8712(11)–2.9068(10) Å, despite the fact that three of the Ru–Ru bonds contain a bridging CO ligand and the other three do not which creates an overall  $D_{3h}$  symmetry. Each Ru atom contains three terminal CO ligands: one that lies in the  $\text{IrRu}_6$

**Received:** August 18, 2011

**Published:** September 15, 2011

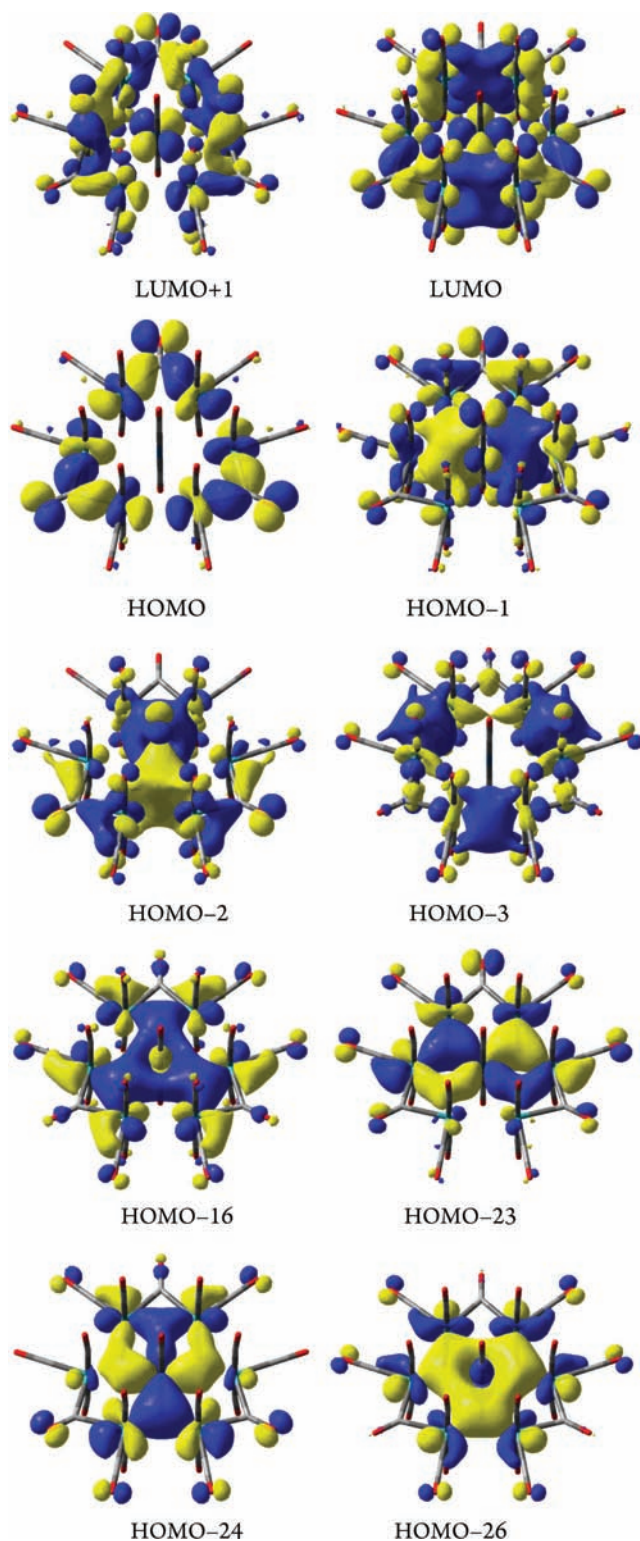


**Figure 2.** Selected molecular orbitals that show the two lowest unoccupied orbitals and the most important metal–metal bonding orbitals for **5**.

plane and two that lie perpendicular to it on opposite sides. The iridium atom contains only two CO ligands that lie on opposite sides and perpendicular to the IrRu<sub>6</sub> plane.

The metal–metal bonding of planar metal clusters frequently violates the traditional electron counting rules, and such is the

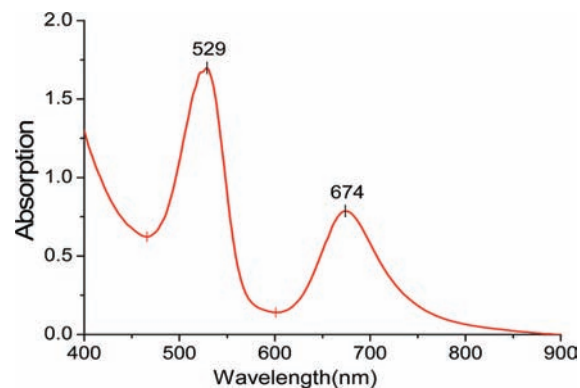


**Figure 3.** UV–vis absorption spectrum of **5** in CH<sub>2</sub>Cl<sub>2</sub> solvent.

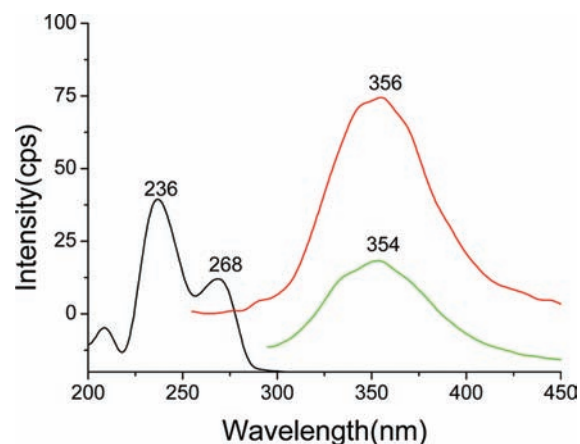


**Figure 4.** Excitation (black, left) and emission spectra for **5** (green, 275 nm excitation; red, 235 nm excitation) in CH<sub>2</sub>Cl<sub>2</sub> solvent.

case with **5**. The anion **5** contains 104 valence electrons while both the EAN rule and the PSEP theory predict a total of 102 electrons for this structure.<sup>1a,12</sup> In order to understand the metal–metal bonding in **5** a series of geometry-optimized DFT molecular orbital calculations were performed.<sup>13</sup> The key molecular orbitals of **5** are shown in Figure 2. The in-plane  $\sigma$ -bonding between the Ir and Ru atoms is nicely represented by the following orbitals:  $a_1'$  HOMO–16, the degenerate  $e'$ , HOMO–23 and HOMO–24, and the  $a_1'$  HOMO–26. The HOMO contains no interactions with the Ir atom and is Ru–Ru antibonding. Although there are significant bonding interactions between the ruthenium atoms and the bridging CO ligands, the HOMO contributes very little to the stabilization of the metal cluster. However, because this orbital is filled, the complex contains two more electrons than expected by the conventional bonding theories.

Complex **5** is highly colored and exhibits two broad absorptions in the visible region of the spectrum; see Figure 3. The absorptions were simulated by time dependent density functional theory (TDDFT) computations.<sup>13</sup> The dominant absorption at 529 nm ( $\epsilon = 15\,640\text{ cm}^{-1}\cdot\text{M}^{-1}$ ) arises from an allowed transition from the  $a_1'$  HOMO–3 to the degenerate  $e'$  LUMO/LUMO+1 pair ( $\lambda_{\text{calcd}} = 525\text{ nm}$ , oscillator strength = 0.3172). This transition may contain an element of metal-to-metal charge transfer from the Ru<sub>6</sub> ring to the central Ir atom, because the HOMO–3 orbital contains no contributions from the Ir atom and the  $E'$  excited state does contain Ir contributions. The broad



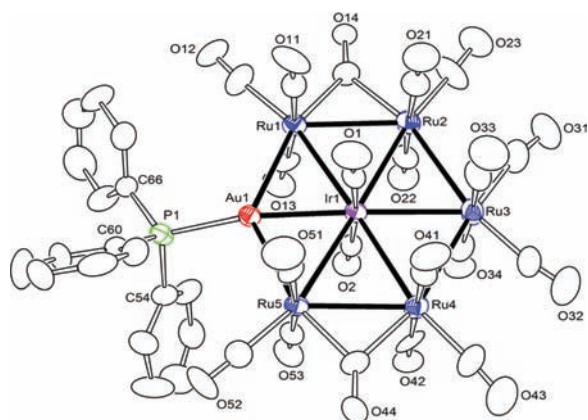


**Figure 5.** An ORTEP diagram of **6** showing 40% thermal probability. Hydrogen atoms have been omitted for clarity. Selected interatomic bond distances (Å) are as follow: Au(1)–Ir(1) = 2.6580(12), Au(1)–Ru(1) = 2.7480(17), Au(1)–Ru(5) = 2.7403(17), Ir(1)–Ru(1) = 2.9080(17), Ir(1)–Ru(2) = 2.9052(17), Ir(1)–Ru(3) = 2.9120(18), Ir(1)–Ru(4) = 2.9057(18), Ir(1)–Ru(5) = 2.9089(16), Ru(1)–Ru(2) = 2.918(2), Ru(2)–Ru(3) = 2.959(2), Ru(3)–Ru(4) = 2.942(2), Ru(4)–Ru(5) = 2.914(2).

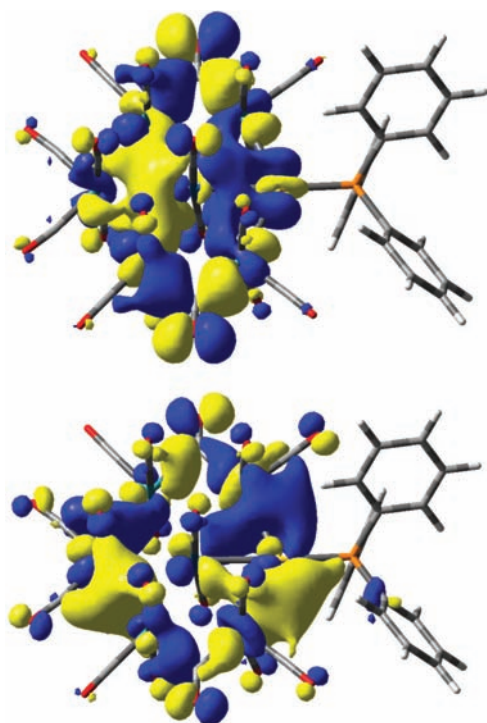
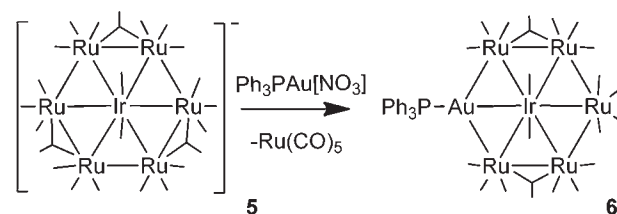


**Figure 6.** Two highest occupied molecular orbitals HOMO (top) and HOMO–1 (bottom) for **6**.

absorption at 674 nm ( $\epsilon = 8180 \text{ cm}^{-1} \cdot \text{M}^{-1}$ ) arises from a transition from the degenerate  $e'$  HOMO–1/HOMO–2 to the  $e'$  LUMO/LUMO+1 pair ( $\lambda_{\text{calcd}} = 705 \text{ nm}$ , oscillator strength = 0.02).

Even more interestingly, anion **5** exhibits a rare luminescence in the 350 nm region when excited with 235 or 275 nm radiation; see Figure 4. Luminescence in metal carbonyl cluster complexes is very rare. In most cases, luminescence by metal carbonyl cluster complexes is created by attaching a luminophore as a

### Scheme 1. Transformation of **5** to **6**



ligand or a tag.<sup>14</sup> The luminescence in **5** may be related to its unusual 2D structure and the existence of delocalized virtual  $\pi$ -orbitals. Calculations to identify the relevant transitions are currently in progress. The related nonplanar anion **4** exhibits no luminescence.

In an attempt to obtain an uncharged derivative of **5**, the anion was treated with  $[\text{PPh}_3\text{Au}][\text{NO}_3]$  in  $\text{CH}_2\text{Cl}_2$  solvent. From this reaction solution, the pink/purple compound  $\text{Ru}_5\text{Ir}(\text{CO})_{20}\text{AuPPh}_3$ , **6**, was isolated. The yield of **6** is low (3%), and there is an intermediate that has not yet been fully characterized.<sup>15</sup> Compound **6** was characterized structurally by a single crystal X-ray diffraction analysis, and an ORTEP diagram of the molecular structure of **6** is shown in Figure 5. All of the metal atoms lie virtually in the same plane. The Au atom exhibits the greatest deviation from the best least-squares plane, 0.140 (1) Å. The Ir–Ru and Ru–Ru distances are similar to those in **5**. The Au–M distances are significantly shorter, Ir(1)–Au(1) = 2.6580(12) Å, Ru(1)–Au(1) = 2.7480(17) Å, Ru(5)–Au(1) = 2.7403(17) Å.

Complex **6** contains only 102 valence electrons, and the HOMO and HOMO–1, Figure 6, show significant in-plane  $\sigma$ - and  $\pi$ -bonding between the Ir and Au atoms that could help to explain the shortness of the Ir–Au bonds. More molecular orbital diagrams showing the interaction between the  $\text{Ru}_5\text{Ir}(\text{CO})_{20}$  and  $\text{AuPPh}_3$  fragments are displayed in the Supporting Information.

The transformation of **5** to **6** is intriguing because it represents the complete replacement of one of the ring  $\text{Ru}(\text{CO})$  groups with a  $\text{Au}(\text{PPh}_3)$  group by the formal elimination of  $\text{Ru}(\text{CO})_5$ ; see Scheme 1 where the CO ligands are shown simply as lines.

Interestingly, compound **6** also exhibits a significant absorption in the visible region of the spectrum: two overlapping absorptions at 494 nm ( $\epsilon = 14082 \text{ cm}^{-1} \cdot \text{M}^{-1}$ ), 520 nm ( $\epsilon = 16858 \text{ cm}^{-1} \cdot \text{M}^{-1}$ ) and one broad absorption at 649 nm ( $\epsilon = 3198 \text{ cm}^{-1} \cdot \text{M}^{-1}$ ); see Figure S2 in the Supporting Information. These absorptions were also accurately simulated by TDDFT calculations; see Figure S6 in the Supporting Information.

As already demonstrated with **3**,<sup>8</sup> it may be possible to fix these 2D clusters on supports and study their catalytic properties. It should also be possible to synthesize complexes related to **5** and **6** having different metal–ligand combinations both in the center of the cluster and in the ring itself that may exhibit interesting absorption and emission properties. These studies are in progress.

### ASSOCIATED CONTENT

**S Supporting Information.** Details of the syntheses and characterizations of the new compounds, computational details, selected molecular orbital diagrams, TDDFT simulated absorption spectra, complete ref 13, and crystallographic details for each

of the structural analyses. This material is available free of charge via the Internet at <http://pubs.acs.org>.

## AUTHOR INFORMATION

### Corresponding Author

Adams@chem.sc.edu; yangxz@berkeley.edu

## ACKNOWLEDGMENT

This research was supported by the National Science Foundation CHE-1111496 (R.D.A.) and the USC Nanocenter. X.Y. gratefully acknowledges support from the National Science Foundation (CHE-0840505) and the Molecular Graphics and Computation Facility (Dr. Kathleen A. Durkin, Director) in the College of Chemistry at the University of California, Berkeley.

## REFERENCES

- (1) (a) Mingos, D. M. P.; May, A. S. In *The Chemistry of Metal Cluster Complexes*; Shriver, D. F., Kaesz, H. D., Adams, R. D.; VCH Publishers: New York, NY, 1990; Chapter 2. (b) Fajardo, M.; Holden, H. D.; Johnson, B. F. G.; Lewis, J.; Raithby, P. R. *J. Chem. Soc., Chem. Commun.* **1984**, 24–25. (c) Schollenberg, M.; Nuber, B.; Ziegler, M. L. *Angew. Chem., Int. Ed.* **1992**, *31*, 350–351. (d) Kong, G.; Harakas, G. N.; Whittlesey, B. R. *J. Am. Chem. Soc.* **1995**, *117*, 3502–3509. (e) Egold, H.; Schraa, M.; Florke, U.; Partyka, J. *Organometallics* **2002**, *21*, 1925–1932. (f) Brayshaw, S. K.; Green, J. C.; Edge, R.; McInnes, E. J. L.; Raithby, P. R.; Warren, J. E.; Weller, A. S. *Angew. Chem., Int. Ed.* **2007**, *46*, 7844–7848.
- (2) Cerrada, E.; Contel, M.; Valencia, A. D.; Laguna, M.; Gelbrich, T.; Hursthouse, M. B. *Angew. Chem., Int. Ed.* **2000**, *39*, 2353–2356.
- (3) Doyle, G.; Eriksen, K. A.; Van Engen, D. *J. Am. Chem. Soc.* **1986**, *108*, 445–451.
- (4) Adams, R. D.; Captain, B.; Hall, M. B.; Trufan, E.; Yang, X. *J. Am. Chem. Soc.* **2007**, *129*, 12328–12340.
- (5) Hungria, A. B.; Raja, R.; Adams, R. D.; Captain, B.; Thomas, J. M.; Midgley, P. A.; Golvenko, V.; Johnson, B. F. G. *Angew. Chem., Int. Ed.* **2006**, *45*, 4782–4785.
- (6) Adams, R. D.; Boswell, E. M.; Captain, B.; Hungria, A. B.; Midgley, P. A.; Raja, R.; Thomas, J. M. *Angew. Chem., Int. Ed.* **2007**, *46*, 8182–8185.
- (7) Adams, R. D.; Blom, D. A.; Captain, B.; Raja, R.; Thomas, J. M.; Trufan, E. *Langmuir* **2008**, *24*, 9223–9226.
- (8) Yang, F.; Trufan, E.; Adams, R. D.; Goodman, D. W. *J. Phys. Chem. C* **2008**, *112*, 14233–14235.
- (9) (a) Waldmann, O. *Coord. Chem. Rev.* **2005**, *249*, 2550–2566. (b) Pizzagalli, L.; Stoeffler, D.; Gautier, F. *Phys. Rev. B* **1996**, *54*, 12216–12224.
- (10) Süß-Fink, G.; Haak, S.; Ferrand, V.; Stoeckli-Evans, H. *J. Chem. Soc., Dalton Trans.* **1997**, 3861–3865.
- (11) Anion **5** can also be obtained from **4** by reaction with one additional equivalent of Ru<sub>3</sub>(CO)<sub>12</sub>.
- (12) Mingos, D. M. P. *Acc. Chem. Res.* **1984**, *17*, 311–319.
- (13) Frisch, M. J. et al. *Gaussian 03, Revision E.01, suite of programs for ab initio calculation*; Gaussian, Inc.: Wallingford, CT, 2004. For complete ref 13, see ref 1 in References for Computational Studies in the Supporting Information.
- (14) (a) Wong, W. Y.; Ting, F. L.; Guo, Y.; Lin, Z. *J. Cluster Sci.* **2005**, *16*, 185–200. (b) Wong, W. Y.; Choi, K. H.; Lin, Z. *Eur. J. Inorg. Chem.* **2002**, 2112–2120. (c) Wong, W. Y.; Wong, W. T. *J. Chem. Soc., Dalton Trans.* **1996**, 1853–1856.
- (15) This purple intermediate exhibits CO absorptions in the IR spectrum in CH<sub>2</sub>Cl<sub>2</sub> (cm<sup>-1</sup>) at 2119(w), 2086(s), 2071(m), 2042(vs), 2030(w,sh), 2010(w), 1976(w), 19955(w,br), 1789(w,br). This compound slowly decomposes to regenerate **5** and small amounts of **6**.